

# The Flow of Power-Law Fluids in Axisymmetric Corrugated Tubes

Taha Sochi\*

June 15, 2010

---

\*University College London, Department of Physics & Astronomy, Gower Street, London, WC1E 6BT. Email: t.sochi@ucl.ac.uk.

# Contents

<b>Contents</b>	<b>2</b>
<b>List of Figures</b>	<b>3</b>
<b>Abstract</b>	<b>4</b>
<b>1 Introduction</b>	<b>5</b>
<b>2 <math>P - Q</math> Relation for Power-Law Fluids</b>	<b>6</b>
2.1 Conic Tube . . . . .	8
2.2 Parabolic Tube . . . . .	9
2.3 Hyperbolic Tube . . . . .	10
2.4 Hyperbolic Cosine Tube . . . . .	10
2.5 Sinusoidal Tube . . . . .	11
<b>3 Conclusions</b>	<b>13</b>
<b>Nomenclature</b>	<b>14</b>
<b>References</b>	<b>15</b>

## List of Figures

1	Profiles of converging-diverging axisymmetric capillaries. . . . .	5
2	The bulk rheology of power-law fluids on logarithmic scales for finite strain rates ( $\dot{\gamma} > 0$ ). . . . .	6
3	Schematic representation of the radius of a conically shaped converging-diverging capillary as a function of the distance along the tube axis. . . . .	8
4	Schematic representation of the radius of a converging-diverging capillary with a parabolic profile as a function of the distance along the tube axis. . . . .	9
5	Schematic representation of the radius of a converging-diverging capillary with a sinusoidal profile as a function of the distance along the tube axis. . . . .	11

# Abstract

In this article we present an analytical method for deriving the relationship between the pressure drop and flow rate in laminar flow regimes, and apply it to the flow of power-law fluids through axially-symmetric corrugated tubes. The method, which is general with regards to fluid and tube shape within certain restrictions, can also be used as a foundation for numerical integration where analytical expressions are hard to obtain due to mathematical or practical complexities. Five converging-diverging geometries are used as examples to illustrate the application of this method.

# 1 Introduction

Modeling the flow in corrugated tubes is required for a number of technological and industrial applications. Moreover, it is a necessary condition for correct description of several phenomena such as yield-stress, viscoelasticity and the flow of Newtonian and non-Newtonian fluids through porous media [1–4]. In the literature of fluid mechanics there are numerous studies on the flow through tubes or channels of corrugated nature. Most of these studies use numerical techniques such as spectral and finite difference methods [1, 5–11]. Some others adopt analytical approaches based on simplified assumptions and normally deal with very special cases [12, 13]. The current paper presents a mathematical method for deriving analytical relations between the volumetric flow rate and pressure drop in corrugated circular capillaries of variable cross section, such as those illustrated schematically in Figure 1. It also presents five examples in which this method is used to derive flow equations for non-Newtonian fluids of power-law rheology. The method, however, is more general and can be used for other tube shapes and other rheologies. The following derivations assume a laminar flow of a purely-viscous incompressible fluid where the tube corrugation is smooth and relatively small to avoid complex flow phenomena which are not accounted for in the underlying assumptions of this method.

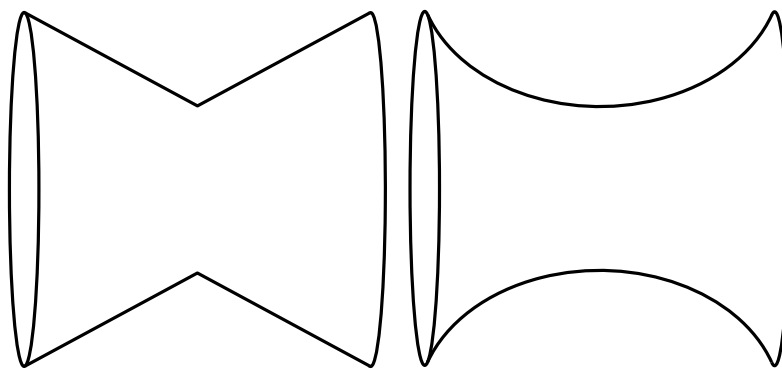


Figure 1: Profiles of converging-diverging axisymmetric capillaries.

## 2 $P - Q$ Relation for Power-Law Fluids

The power-law, or Ostwald-de Waele, is a widely-used fluid model to describe the rheology of shear thinning fluids. It is one of the simplest time-independent non-Newtonian models as it contains two parameters only. The model is given by the relation [14, 15]

$$\mu = \frac{\tau}{\dot{\gamma}} = C\dot{\gamma}^{n-1} \quad (1)$$

where  $\mu$  is the fluid viscosity,  $\tau$  is the stress,  $\dot{\gamma}$  is the strain rate,  $C$  is the consistency factor, and  $n$  is the flow behavior index. In Figure 2 the bulk rheology of this model for shear-thinning case is presented generically on log-log scales. Although the power-law is used to model shear-thinning fluids, it can also be used for modeling shear-thickening by making  $n$  greater than unity. The major weakness of power-law model is the absence of plateaux at low and high strain rates. Consequently, it fails to produce sensible results in these flow regimes.

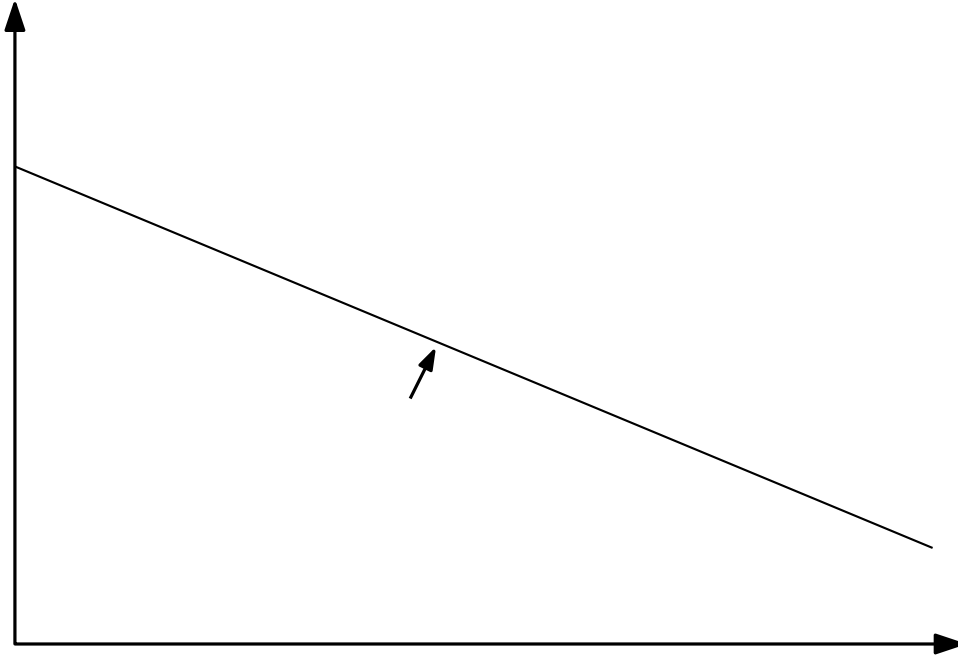


Figure 2: The bulk rheology of power-law fluids on logarithmic scales for finite strain rates ( $\dot{\gamma} > 0$ ).

The volumetric flow rate,  $Q$ , of a power law fluid through a circular capillary of constant radius  $r$  with length  $x$  across which a pressure drop  $P$  is applied is given by

$$Q = \frac{\pi n r^4 P^{1/n}}{2x C^{1/n} (3n+1)} \left( \frac{2x}{r} \right)^{1-1/n} \quad (2)$$

A derivation of this relation, which can be obtained from Equation 1, can be found in [16, 17]. On solving this equation for  $P$  the following relation is obtained

$$P = \frac{2CQ^n(3n+1)^n x}{\pi^n n^n r^{3n+1}} \quad (3)$$

For an infinitesimal length,  $\delta x$ , of a capillary, the infinitesimal pressure drop for a given flow rate  $Q$  is

$$\delta P = \frac{2CQ^n(3n+1)^n \delta x}{\pi^n n^n r^{3n+1}} \quad (4)$$

For an incompressible fluid, the volumetric flow rate across an arbitrary cross section of the capillary is constant. Therefore, the total pressure drop across a capillary of length  $L$  with circular cross section of varying radius,  $r(x)$ , is given by

$$P = \frac{2CQ^n(3n+1)^n}{\pi^n n^n} \int_0^L \frac{dx}{r^{3n+1}} \quad (5)$$

In the following sections, Equation 5 will be used to derive analytical expressions for the relation between pressure drop and volumetric flow rate for five converging-diverging geometries of axially-symmetric pipes. The method can be equally applied to other geometries as long as the tube radius can be expressed analytically as a function of the tube axial distance.

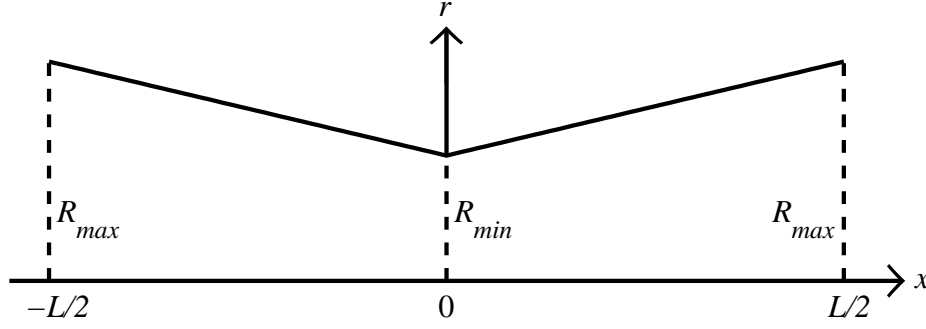


Figure 3: Schematic representation of the radius of a conically shaped converging-diverging capillary as a function of the distance along the tube axis.

## 2.1 Conic Tube

For a corrugated tube of conic shape, depicted in Figure 3, the radius  $r$  as a function of the axial coordinate  $x$  in the designated frame is given by

$$r(x) = a + b|x| \quad -L/2 \leq x \leq L/2 \quad a, b > 0 \quad (6)$$

where

$$a = R_{min} \quad \text{and} \quad b = \frac{2(R_{max} - R_{min})}{L} \quad (7)$$

Hence, Equation 5 becomes

$$P = \frac{2CQ^n(3n+1)^n}{\pi^n n^n} \int_{-L/2}^{L/2} \frac{dx}{(a + b|x|)^{3n+1}} \quad (8)$$

$$= \frac{2CQ^n(3n+1)^n}{\pi^n n^n} \left( \left[ \frac{1}{3bn(a - bx)^{3n}} \right]_{-L/2}^0 + \left[ -\frac{1}{3bn(a + bx)^{3n}} \right]_0^{L/2} \right) \quad (9)$$

$$= \frac{4CQ^n(3n+1)^n}{3\pi^n n^{n+1}b} \left[ \frac{1}{a^{3n}} - \frac{1}{(a + bL/2)^{3n}} \right] \quad (10)$$

that is

$$P = \frac{2LCQ^n(3n+1)^n}{3\pi^n n^{n+1}(R_{max} - R_{min})} \left[ \frac{1}{R_{min}^{3n}} - \frac{1}{R_{max}^{3n}} \right] \quad (11)$$



## 2.2 Parabolic Tube

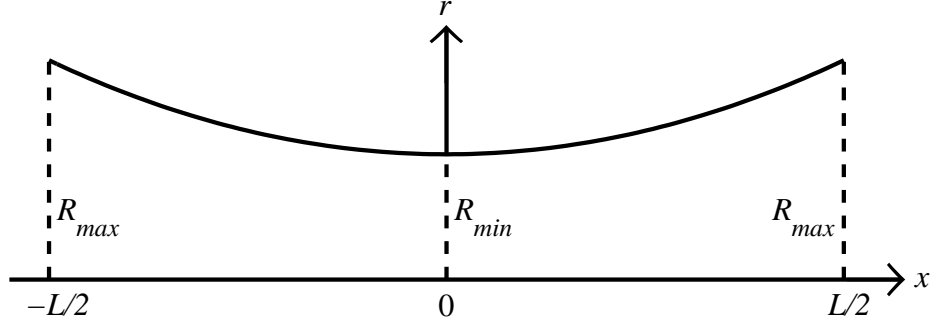


Figure 4: Schematic representation of the radius of a converging-diverging capillary with a parabolic profile as a function of the distance along the tube axis.

For a tube of parabolic profile, depicted in Figure 4, the radius is given by

$$r(x) = a + bx^2 \quad -L/2 \leq x \leq L/2 \quad a, b > 0 \quad (12)$$

where

$$a = R_{min} \quad \text{and} \quad b = \left(\frac{2}{L}\right)^2 (R_{max} - R_{min}) \quad (13)$$

Therefore, Equation 5 becomes

$$P = \frac{2CQ^n(3n+1)^n}{\pi^n n^n} \int_{-L/2}^{L/2} \frac{dx}{(a + bx^2)^{3n+1}} \quad (14)$$

$$= \frac{2CQ^n(3n+1)^n}{\pi^n n^n a} \left[ x \left( \frac{bx^2}{a} + 1 \right)^{3n} {}_2F_1 \left( \frac{1}{2}, 3n+1; \frac{3}{2}; -\frac{bx^2}{a} \right) \right]_{-L/2}^{L/2} \quad (15)$$

where  ${}_2F_1$  is the hypergeometric function. Therefore

$$P = \frac{2LCQ^n(3n+1)^n}{n^n \pi^n R_{min}^{3n+1}} {}_2F_1 \left( \frac{1}{2}, 3n+1; \frac{3}{2}; 1 - \frac{R_{max}}{R_{min}} \right) \quad (16)$$

## 2.3 Hyperbolic Tube

For a tube of hyperbolic profile, similar to the profile in Figure 4, the radius is given by

$$r(x) = \sqrt{a + bx^2} \quad -L/2 \leq x \leq L/2 \quad a, b > 0 \quad (17)$$

where

$$a = R_{min}^2 \quad \text{and} \quad b = \left(\frac{2}{L}\right)^2 (R_{max}^2 - R_{min}^2) \quad (18)$$

Therefore, Equation 5 becomes

$$P = \frac{2CQ^n(3n+1)^n}{\pi^n n^n} \int_{-L/2}^{L/2} \frac{dx}{(a + bx^2)^{(3n+1)/2}} \quad (19)$$

$$= \frac{2CQ^n(3n+1)^n}{\pi^n n^n} \left[ x \left( \frac{\frac{bx^2}{a} + 1}{a + bx^2} \right)^{\frac{3n+1}{2}} {}_2F_1 \left( \frac{1}{2}, \frac{3n+1}{2}; \frac{3}{2}; -\frac{bx^2}{a} \right) \right]_{-L/2}^{L/2} \quad (20)$$

where  ${}_2F_1$  is the hypergeometric function. Therefore

$$P = \frac{2LCQ^n(3n+1)^n}{\pi^n n^n R_{min}^{3n+1}} {}_2F_1 \left( \frac{1}{2}, \frac{3n+1}{2}; \frac{3}{2}; 1 - \frac{R_{max}^2}{R_{min}^2} \right) \quad (21)$$

## 2.4 Hyperbolic Cosine Tube

For a tube of hyperbolic cosine profile, similar to the profile in Figure 4, the radius is given by

$$r(x) = a \cosh(bx) \quad -L/2 \leq x \leq L/2 \quad a > 0 \quad (22)$$

where

$$a = R_{min} \quad \text{and} \quad b = \frac{2}{L} \operatorname{arccosh} \left( \frac{R_{max}}{R_{min}} \right) \quad (23)$$

Hence, Equation 5 becomes

$$P = \frac{2CQ^n(3n+1)^n}{\pi^n n^n a^{3n+1}} \int_{-L/2}^{L/2} \frac{dx}{\cosh^{3n+1}(bx)} \quad (24)$$

$$= \frac{2CQ^n(3n+1)^n}{3\pi^n n^{n+1} a^{3n+1} b} \left[ \frac{\sinh(bx)}{\cosh^{3n}(bx) \sqrt{-\sinh^2(bx)}} {}_2F_1 \left( \frac{1}{2}, -\frac{3n}{2}; \frac{2-3n}{2}; \cosh^2(bx) \right) \right]_{-L/2}^{L/2} \quad (25)$$

On evaluating the last expression and taking its real part which is physically significant, the following relation is obtained

$$P = \frac{2LCQ^n(3n+1)^n}{3\pi^n n^{n+1} R_{min} R_{max}^{3n} \operatorname{arccosh} \left( \frac{R_{max}}{R_{min}} \right)} \operatorname{Im} \left( {}_2F_1 \left( \frac{1}{2}, -\frac{3n}{2}; \frac{2-3n}{2}; \frac{R_{max}^2}{R_{min}^2} \right) \right) \quad (26)$$

where  $\operatorname{Im}({}_2F_1)$  is the imaginary part of the hypergeometric function.

## 2.5 Sinusoidal Tube

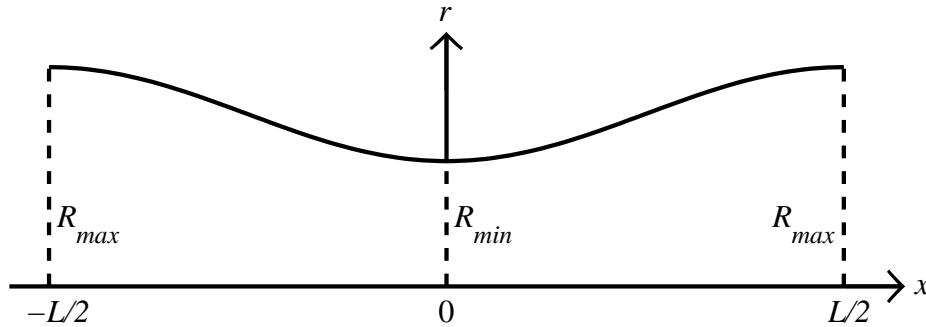


Figure 5: Schematic representation of the radius of a converging-diverging capillary with a sinusoidal profile as a function of the distance along the tube axis.

For a tube of sinusoidal profile, depicted in Figure 5, where the tube length  $L$  spans one complete wavelength, the radius is given by

$$r(x) = a - b \cos(kx) \quad -L/2 \leq x \leq L/2 \quad a > b > 0 \quad (27)$$

where

$$a = \frac{R_{max} + R_{min}}{2} \quad b = \frac{R_{max} - R_{min}}{2} \quad \& \quad k = \frac{2\pi}{L} \quad (28)$$

Hence, Equation 5 becomes

$$P = \frac{2CQ^n(3n+1)^n}{\pi^n n^n} \int_{-L/2}^{L/2} \frac{dx}{[a - b \cos(kx)]^{3n+1}} \quad (29)$$

$$= -\frac{2CQ^n(3n+1)^n}{3\pi^n n^{n+1}k} \left[ \frac{1}{\sin(kx) [a - b \cos(kx)]^{3n}} \sqrt{\frac{-\sin^2(kx)}{a^2 - b^2}} \mathfrak{A} \right]_{-L/2}^{L/2} \quad (30)$$

where  $\mathfrak{A}$  is the Appell hypergeometric function given by

$$\mathfrak{A} = F_1 \left( -3n; \frac{1}{2}, \frac{1}{2}; 1 - 3n; \frac{a - b \cos(kx)}{a + b}, \frac{a - b \cos(kx)}{a - b} \right) \quad (31)$$

On taking the limit as  $x \rightarrow -\frac{L}{2}^+$  and  $x \rightarrow \frac{L}{2}^-$  and considering the real part, the following relation is obtained

$$P = \frac{2LCQ^n(3n+1)^n}{3\pi^{n+1}n^{n+1}R_{max}^{3n}\sqrt{R_{max}R_{min}}} \text{Im} \left( F_1 \left( -3n; \frac{1}{2}, \frac{1}{2}; 1 - 3n; 1, \frac{R_{max}}{R_{min}} \right) \right) \quad (32)$$

where  $\text{Im}(F_1)$  is the imaginary part of the Appell hypergeometric function.

It is noteworthy that all these relations (i.e. Equations 11, 16, 21, 26 and 32), are dimensionally consistent. Moreover, they have been thoroughly tested and validated by numerical integration.

### 3 Conclusions

In this article a mathematical method for obtaining analytical relations between the flow rate and pressure drop in axisymmetric corrugated tubes is presented and applied to the flow of power-law fluids. The method is illustrated by five examples of circular capillaries with converging-diverging shape. This method can be used to derive similar relations for other types of fluid and other types of tube geometry. It can also be used as a base for numerical integration where analytical relations are difficult to obtain due to mathematical or practical reasons.

## Nomenclature

$\dot{\gamma}$	strain rate ( $\text{s}^{-1}$ )
$\mu$	fluid viscosity (Pa.s)
$\tau$	stress (Pa)
$C$	consistency factor ( $\text{Pa.s}^n$ )
$F_1$	Appell hypergeometric function
${}_2F_1$	hypergeometric function
$L$	tube length (m)
$n$	flow behavior index
$P$	pressure drop (Pa)
$Q$	volumetric flow rate ( $\text{m}^3.\text{s}^{-1}$ )
$r$	tube radius (m)
$R_{max}$	maximum radius of corrugated tube (m)
$R_{min}$	minimum radius of corrugated tube (m)
$x$	axial coordinate (m)

## References

- [1] S. Pilitsis; A.N. Beris. Calculations of steady-state viscoelastic flow in an undulating tube. *Journal of Non-Newtonian Fluid Mechanics*, 31(3):231–287, 1989. [5](#)
- [2] K.K. Talwar; B. Khomami. Application of higher order finite element methods to viscoelastic flow in porous media. *Journal of Rheology*, 36(7):1377–1416, 1992. [5](#)
- [3] T. Sochi. Pore-scale modeling of viscoelastic flow in porous media using a Bautista-Manero fluid. *International Journal of Heat and Fluid Flow*, 30(6):1202–1217, 2009. [5](#)
- [4] T. Sochi. Modelling the flow of yield-stress fluids in porous media. *Transport in Porous Media*, 2010. DOI: 10.1007/s11242-010-9574-z. [5](#)
- [5] N. Phan-Thien; C.J. Goh; M.B. Bush. Viscous flow through corrugated tube by boundary element method. *Journal of Applied Mathematics and Physics (ZAMP)*, 36(3):475–480, 1985. [5](#)
- [6] N. Phan-Thien; M.M.K. Khan. Flow of an Oldroyd-type fluid through a sinusoidally corrugated tube. *Journal of Non-Newtonian Fluid Mechanics*, 24:203–220, 1987. [5](#)
- [7] A. Lahbabi; H-C Chang. Flow in periodically constricted tubes: Transition to inertial and nonsteady flows. *Chemical Engineering Science*, 41(10):2487–2505, 1986. [5](#)
- [8] S.R. Burdette; P.J. Coates; R.C. Armstrong; R.A. Brown. Calculations of viscoelastic flow through an axisymmetric corrugated tube using the explicitly

- elliptic momentum equation formulation (EEME). *Journal of Non-Newtonian Fluid Mechanics*, 33(1):1–23, 1989. [5](#)
- [9] S. Pilitsis; A.N. Beris. Pseudospectral calculations of viscoelastic flow in a periodically constricted tube. *Computer Methods in Applied Mechanics and Engineering*, 98(3):307–328, 1992. [5](#)
- [10] D.F. James; N. Phan-Thien; M.M.K. Khan; A.N. Beris; S. Pilitsis. Flow of test fluid M1 in corrugated tubes. *Journal of Non-Newtonian Fluid Mechanics*, 35(2-3):405–412, 1990. [5](#)
- [11] S.H. Momeni-Masuleh; T.N. Phillips. Viscoelastic flow in an undulating tube using spectral methods. *Computers & fluids*, 33(8):1075–1095, 2004. [5](#)
- [12] S. Oka. Pressure development in a non-Newtonian flow through a tapered tube. *Rheologica Acta*, 12(2):224–227, 1973. [5](#)
- [13] E.W. Williams; S.H. Javadpour. The flow of an elastico-viscous liquid in an axisymmetric pipe of slowly varying cross-section. *Journal of Non-Newtonian Fluid Mechanics*, 7(2-3):171–188, 1980. [5](#)
- [14] R.B. Bird; R.C. Armstrong; O. Hassager. *Dynamics of Polymeric Liquids*, volume 1. John Wiley & Sons, second edition, 1987. [6](#)
- [15] P.J. Carreau; D. De Kee; R.P. Chhabra. *Rheology of Polymeric Systems*. Hanser Publishers, 1997. [6](#)
- [16] T. Sochi; M.J. Blunt. Pore-scale network modeling of Ellis and Herschel-Bulkley fluids. *Journal of Petroleum Science and Engineering*, 60(2):105–124, 2008. [7](#)
- [17] T. Sochi. *Pore-Scale Modeling of Non-Newtonian Flow in Porous Media*. PhD thesis, Imperial College London, 2007. [7](#)